

# Triangularly phase-modulated optical fiber ring resonator sensor

Pie-Yau Chien and Ci-Ling Pan

An optical fiber ring resonatory sensor system has been demonstrated by applying a triangular phase modulation signal to a fiber loop. The dynamic range for detection of optical phase change is  $2\pi$ . The sensor is linear within this range. The minimum detectable optical phase change is  $1.5 \times 10^{-4}$  rad/Hz<sup>1/2</sup>.

*Key words:* Fiber resonator, sensor, signal processing.

## I. Introduction

The optical fiber ring resonator has been extensively studied by many workers for a number of years.<sup>1-14</sup> This optical device has been used for sensor applications,<sup>7</sup> laser-diode frequency stabilization,<sup>8</sup> and in fiber-optic gyroscopes.<sup>9-14</sup> In these applications, in order to obtain a highly sensitive output signal for a given change in the optical path length or laser frequency, the linewidth of the resonator is in general the most important parameter. The intensity variation at the maximum sensitive position of the transmittance of the resonator<sup>7,8</sup> or a differential S-shaped output signal obtained at the resonance frequency<sup>9</sup> has been used to extract information on the change in optical phase delay. The ring resonator is more sensitive than Mach-Zehnder-type interferometers, but its dynamic range and linearity characteristics are limited by the resonator linewidth and thus are inferior to Mach-Zehnder-type interferometers. To alleviate this problem, one can employ the so-called closed-loop configuration often used in fiber-optic gyroscopes.<sup>10-14</sup> In this method, two acousto-optic modulators operated as frequency shifters are used to tune the laser frequency to the peak position of the resonance curve. The optical phase change is then nulled by tuning the laser frequency. The dynamic range and the linearity of the discrimination curve is then no longer limited by the FWHM linewidth of the ring resonator, but by the maximum tuning range of the laser frequency. Recently, we demonstrated a

frequency stabilizer for a set of laser diodes by applying a triangular phase modulation signal to a bulk Fabry-Perot interferometer followed by a time-gating technique<sup>15</sup> for signal processing. Because of a linearly scanned optical phase delay by a triangular waveform, the dynamic range of the frequency discriminator is thus improved. In this paper we apply this technique to signal processing in a fiber ring resonator. It is shown that the linearity and dynamic range of the sensor system are improved significantly. In Section II the basic principle of our approach is described. The experimental method is discussed in Section III. Finally, experimental results are presented and discussed in Section IV.

## II. Basic Principles

A fiber-optic ring resonator interferometer is simply a ring section of a single-mode fiber with a fiber coupler exhibiting a highly unbalanced coupling ratio. The free spectral range (FSR) of the resonator is  $c/nL_0$ , where  $L_0$  is the length of the ring resonator and  $n$  is the refractive index of the fiber core. Its characteristics are similar to a bulk Fabry-Perot interferometer in which the reflected power exhibits sharp minima at resonance. The relation between the output intensity  $I_o$  and the input intensity  $I_i$  of a fiber-optic ring resonator can be expressed as<sup>1</sup>

$$I_o/I_i = (1 - \gamma_o) \times [1 - (1 - K_r)/(1 + K_r)^2 - 4K_r \sin^2(\beta L/2 - \pi/4)], \quad (1)$$

where  $\gamma_o$  and  $K_r$  are, respectively, the fractional loss and the coupling coefficient of the fiber coupler. Under the condition that  $\beta L = m(2\pi) - \pi/2$ , such that  $\sin^2[(\beta L/2 - \pi/4)] = 1$  in Eq. (1), the output intensity of the fiber resonator is then at its minimum.

The authors are with the Institute of Electro-Optical Engineering, National Chiao-Tung University, Hsinchu, Taiwan 30050, China.

Received 18 September 1990.

0003-6935/92/152776-04\$05.00/0.

© 1992 Optical Society of America.

To sense the change in fiber length, we applied a triangular phase modulation signal to a fiber-coiled piezoelectric transducer (PZT) in the fiber loop, so that the optical phase delay is swept linearly as shown in Fig. 1. The amplitude of the triangular waveform is adjusted such that the sweeping range is equal to one FSR. The output of the resonator contains one spectral line corresponding to that of a single-mode laser within the sweeping time, as shown in Fig. 1(b). If the resonance condition is further satisfied, the optical phase delay within the two half-periods of the triangular waveform can be expressed as

$$\phi_+ = \beta(L_o + L_s + \gamma t) = 2m\pi, \quad -T/2 < t < 0, \quad (2a)$$

and

$$\phi_- = \beta(L_o + L_s - \gamma t) = 2m\pi, \quad 0 < t < +T/2, \quad (2b)$$

where  $L_o$  is the bias fiber length;  $L_s$  is the change in fiber length to be measured;  $\phi_b \equiv \beta L_o$ ;  $\phi_s \equiv \beta L_s$ ;  $\gamma$  is the slope of the triangular waveform; and  $m = 0, 1, 2, 3, \dots$ . By differentiating between Eqs. (2a) and (2b) with respect to  $L_s$  and  $t$ , we can derive the positions of the spectral lines in the time domain. These are

$$\Delta t_+ = -\Delta L_s / \gamma, \quad -T/2 < t < 0, \quad (3a)$$

$$\Delta t_- = +\Delta L_s / \gamma, \quad 0 < t < +T/2. \quad (3b)$$

The time intervals,  $\Delta t_+$  and  $\Delta t_-$ , can be detected, respectively, by the gate-switching technique.<sup>15</sup> The temporal separation of these lines in the two half-periods of a triangular waveform is

$$\Delta t_d = |\Delta t_+ - \Delta t_-| = 2\Delta L_s / \gamma. \quad (4)$$

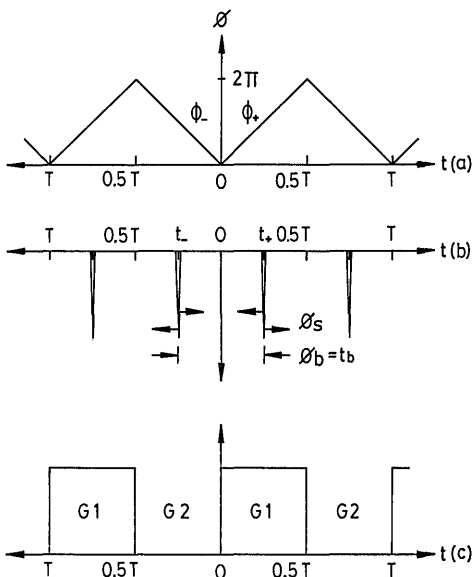


Fig. 1. Operating principle of the triangular phase-modulated fiber ring resonator sensor: (a) triangular phase modulation waveform; (b) corresponding spectral lines in positive- and negative-sloped regions of the triangular waveform, where  $\phi_b \equiv \beta L_o$  and  $\phi_s \equiv \beta L_s$ ; (c) gate-switching signal for spectral line selection.

It follows that the path-length change,  $\Delta L_s$ , can be measured directly from the time difference,  $\Delta t_d$ . This can be measured either from the analog output of a phase meter or digitally by using a gated counter. Since  $\Delta t_d$  is linearly related to the optical phase change within the full  $2\pi$  rad phase range, the full FSR of the resonator is available for measurement in our system. In contrast, the region that can be used for path-length measurement in conventional methods<sup>7-9</sup> is equal to the FWHM of the resonance curve, which is inversely proportional to the finesse.

### III. Experimental Method

Our experimental setup is shown in Fig. 2. The light source was a single-mode laser diode (Hitachi Model HLP1400,  $\lambda = 0.83 \mu\text{m}$ ), for which the driving current and operating temperature were both stabilized such that  $\Delta I_o / I_o \leq 1.0 \times 10^{-5}$  and  $\Delta T \leq 1.0 \times 10^{-3} \text{C}$ . An optical fiber ring resonator loop was constructed with an adjustable fiber coupler and a fiber section. Nonpolarization-maintaining, single-mode, 30-cm long fiber was used in this experiment. By adjusting the coupling ratio of the adjustable fiber coupler, we obtained a finesse of 70 for our resonator. Two in-line fiber polarization controllers (PC's), one placed at the input port of the fiber coupler and the other located in the fiber loop, were used such that the fiber loop operated in the true single polarization mode. Two fiber-coiled piezoelectric transducers, PZT1 and PZT2, were used for signal processing. The PZT1 was used to sweep linearly the optical phase delay at 30 kHz and stabilize the operation bias points. The PZT2 was used to simulate a change in fiber length for system performance test. The amplitude of the triangular waveform applied to PZT1 was adjusted such that only one spectral line was observed in each of the two half-periods of the triangular waveform. This output signal was then gate switched to select the spectral lines in the two half-periods. The time difference between these two gated output signals was then compared at the phase meter. The optical path length

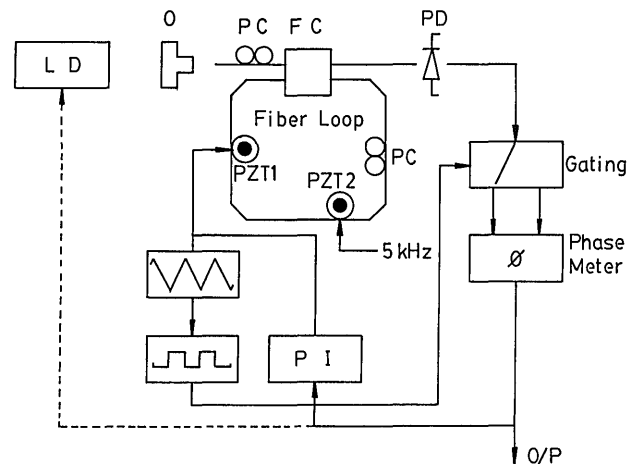


Fig. 2. Experimental setup: LD, laser diode; O, objective lens; PC, polarization controller; FC, fiber coupler; PD, photodetector; PZT, piezoelectric transducer; PI, proportional and integrating circuit.

can be detected by measuring the time delay or the phase difference of these gated signals.

#### IV. Results and Discussions

The output signals of the fiber ring resonator at the photodiode are shown in Figs. 3(a) and 3(b) for different path-length differences. It is clear that the change in optical phase delay manifests itself as different time delay positions. In order to eliminate the low-frequency, environmentally induced optical phase noise, the output signal of the phase meter at a frequency lower than 1.0 kHz was used for stabilization of the operation bias point. To achieve this, the output signal of the phase meter was sent through a proportional and integrating (P + I) circuit and then applied to PZT1. In order to achieve the maximum possible dynamic range of the sensor output, the bias point of the ring resonator can be stabilized such that the spectral lines are located at the central positions of the two sweeping half-periods. This can be achieved by controlling the fiber length, e.g., the spectral line located at  $T/4$  for the positively ramped modulation signal and  $-T/4$  for the negative ramped modulation signal. For measurement of the time difference,  $\Delta t_d$ , a gating signal can be generated from the triangular waveform and used to select the two spectral lines located on the positive-sloped and negative-sloped

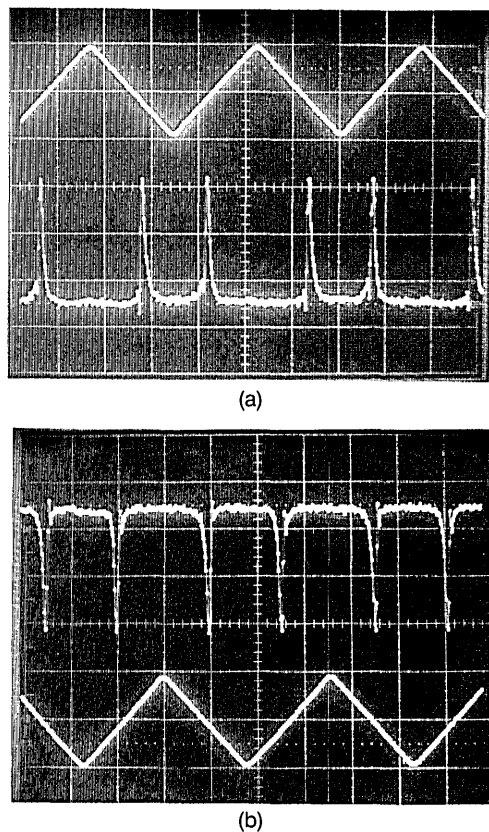


Fig. 3. (a), (b) Photodiode output signals for two different optical phase biases. The upper trace represents the detected signal; the lower trace represents the applied triangular phase modulation signal. The peak-to-peak voltage of the triangular waveform is 1.2 V and its frequency is 30 kHz.

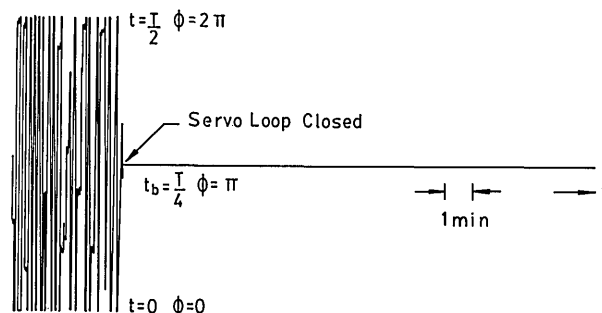


Fig. 4. Phase meter output with a feedback loop for operation bias point stabilization under free-running and closed-loop conditions. The optical phase delay is stabilized at  $\phi = \pi$ , corresponding to a time delay of  $t_b = T/4$ .

regions of the triangular waveform as shown in Fig. 1(c). The time difference can then be read out by a phase meter at the output of the gate switches. In our system, the servo bandwidth was selected to be 1.0 kHz, the optical phase bias,  $\phi_b$ , of the phase delays,  $\phi_+$  and  $\phi_-$ , has been stabilized to  $\Delta\phi_b \leq 1.5 \times 10^{-4}$  rad/Hz<sup>1/2</sup>. Following Eqs. (2)–(4), we find that the corresponding timing jitter is  $\Delta t_d \leq 0.36$  ns as predicted by Eq. (4). The minimum detectable fiber length change is  $\Delta L_{\min} = (\Delta\phi_{b,\min} \times \lambda) / (n \times 2\pi) \cong 1.3$  nm, where  $\lambda$  is the wavelength of the laser diode and  $n$  is the refractive index of the single-mode fiber. This result is shown in Fig. 4 for the free-running and closed-loop situations.

The linearity of the system response is influenced by the linearity of the PZT. At the turning point of the triangular waveform, high frequency harmonics of the modulation signal are present, and the frequency response of the PZT may not be high enough to respond. This problem can be eliminated by modifying the duty cycle of the gate-switching waveform such that the nonlinear region is gated out. If the temperature of the fiber loop is also stabilized, this

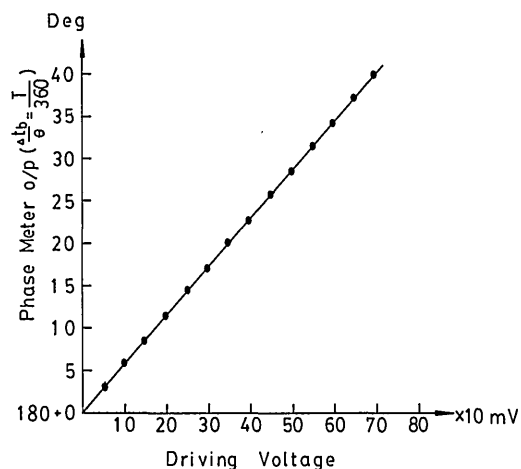


Fig. 5. Phase meter output as a function of the amplitude of a 5-kHz sinusoidal waveform applied to PZT2. The relation between the phase meter output  $\theta$  and the temporal separation  $\Delta t_d$  of the spectral lines in the two half-periods of the triangular waveform is  $\theta = (360^\circ/T) \times \Delta t_d$ , where  $T$  is the period of the triangular waveform.

system can be used as the frequency discriminator of the laser diode. The long-term frequency stability achievable, however, is influenced by the change and slow drift in the PZT response. The frequency discriminating characteristics of our approach were obtained from the symmetrical positions in the two half-periods of the triangular waveform. Thus common mode noise resulting from the PZT can be partially eliminated. Figure 5 shows the result of the scale factor linearity of the sensor system with a 5.0-kHz modulation signal applied to PZT2.

#### IV. Conclusion

We have demonstrated a novel technique for signal processing in fiber ring resonator sensors, based on a triangular phase modulation waveform. The change in optical path length was measured by the time difference between the positions of the spectral lines in two half-periods of the triangular signal. The minimum detectable optical phase delay was  $1.5 \times 10^{-4}$  rad/Hz<sup>1/2</sup>. The dynamic range in the phase delay of the system is  $2\pi$  rad.

This work was partially supported by the National Science Council of the Republic of China under grant NSC-80-0417-009-05.

#### References

1. L. F. Stokes, M. Chodorow, and H. J. Shaw, "All-single-mode fiber resonator," *Opt. Lett.* **7**, 288–290 (1982).
2. E. J. Bachus, R. P. Braun, and B. Streb, "Polarization maintaining single-mode-fiber resonator," *Electron. Lett.* **19**, 1027–1028 (1983).
3. L. F. Stokes, M. Chodorow, and H. J. Shaw, "All-fiber stimulated Brillouin ring laser with submilliwatt pump threshold," *Opt. Lett.* **7**, 509–511 (1982).
4. E. Desurvire, M. J. F. Digonnet, and H. J. Shaw, "Theory and implementation of a Raman active delay line," *IEEE J. Lightwave Technol.* **LT-4**, 426–443 (1986).
5. E. Desurvire, A. Imamoglu, and H. J. Shaw, "Low threshold synchronously pump all fiber ring Raman laser," *IEEE J. Lightwave Technol.* **LT-5**, 89–96 (1987).
6. M. V. Andres and K. W. H. Foulds, "Optical-fiber resonator rings based on polarization-dependent coupler," *IEEE J. Lightwave Technol.* **8**, 1212–1225 (1990).
7. L. F. Stokes, M. Chodorow, and H. J. Shaw, "Sensitive all single-mode fiber resonant ring interferometer," *IEEE J. Lightwave Technol.* **LT-1**, 110–115 (1983).
8. S. Tai, K. Kyuma, and T. Nakayama, "Spectrum linewidth of an external cavity laser diode stabilized by a fiber ring resonator," *Appl. Phys. Lett.* **47**, 91–93 (1985).
9. M. Ohtsu and S. Araki, "Using a 1.5- $\mu$ m DFB InGaAsP laser in a passive ring cavity-type fiber gyroscope," *Appl. Opt.* **26**, 464–470 (1987).
10. R. E. Meyer, S. Ezekiel, D. W. Stone, and V. J. Tekippe, "Passive fiber-optic ring resonator for rotation sensing," *Opt. Lett.* **8**, 644–646 (1983).
11. Y. Ohtsuka, "Analysis of a fiber-optic passive loop resonator gyroscope: dependence on resonator parameters and light source coherence," *IEEE J. Lightwave Technol.* **LT-3**, 378–384 (1985).
12. K. Iwatsuki, K. Hotate, and M. Higashiguchi, "Effect of Rayleigh backscattering on an optical passive ring-resonator gyro," *Appl. Opt.* **23**, 3916–3924 (1984).
13. K. Iwatsuki, K. Hotate, and M. Higashiguchi, "Kerr effect in an optical passive-resonator gyro," *IEEE J. Lightwave Technol.* **LT-4**, 645–651 (1986).
14. K. Iwatsuki, K. Hotate, and M. Higashiguchi, "Backscattering in an optical passive ring-resonator gyro: experiment," *Appl. Opt.* **25**, 4448–4451 (1986).
15. P. Y. Chien and C. L. Pan, "Relative frequency stabilization of a set of laser diodes using the time-gating technique," *Opt. Commun.* **83**, 81–84 (1991).